2010

Inversion-based feedforward control of polypyrrole trilayer bender actuators

Stephen W. John
University of Wollongong, swj56@uow.edu.au

Gursel Alici
University of Wollongong, gursel@uow.edu.au

Christopher David Cook
University of Wollongong, chris_cook@uow.edu.au

Inversion-Based Feedforward Control of Polypyrrole Trilayer Bender Actuators

Stephen W. John, Gursel Alici, and Christopher D. Cook

***Abstract*—Conducting polymer bending actuators show potential for unique manipulation devices, particularly at the microscale, given low actuation voltages, controllable manufacture, biocompatibility, and ability to operate in either air or liquid environments; however, the impracticalities of implementing feedback in these environments and at these scales can impede positional control of the actuator. This paper presents an application of inversion-based feedforward positional control to a trilayer bender actuator, which is shown to improve the performance without the use of feedback or adjustments to the chemistry of the device. The step and dynamic displacement responses have all been improved under the feedforward control system, while the response does not change significantly under large increases in external loads. This study contributes the first implementation of inversion-based feedforward control to the emerging area of conducting polymer actuators, paving the way toward their use in functional devices, particularly where the implementation of feedback is difficult.**

***Index Terms*—Actuators, feedforward systems, intelligent materials, modeling.**

I. Introduction

ACTUATORS based on conducting polymers, such as polypyrrole, are an emerging type of device and are attractive for many applications given their low actuation voltage, biocompatibility, and their ability to operate in air and liquid environments [1], [2]. These devices utilize the volume change (or strain) of a conducting polymer in response to an applied voltage, and may produce linear movement when used in isolation, or bending movement when combined with an inert layer. Bending actuators, based on the conducting polymer polypyrrole (PPy), also show potential for microscale applications given the controllable manufacture of devices on that scale [3] and their demonstrated manipulation of microscale objects [4]–[6]. Despite this progress on the manufacture of polypyrrole actuators, both on the macro- and microscale, there are limitations to their use, with large time constants [7]–[9], unknown system dynamics, and positional drift over longer time periods [4], [10]. Hysteresis in the displacement of trilayer actuators has been suggested to be minor [4], although more characterization is required. Modification of the actuator chemistry, particularly the dopant, has been shown to improve the speed and magnitude of polypyrrole films actuation [11]–[13]. Applying control techniques to the actuator displacement shows strong potential for further performance improvement without adjusting the chemistry.

The application of traditional control strategies to conducting polymer bending actuators has been limited. Yao *et al.* [14] have applied a PID control methodology to improve the rise time of a bender by up to 500 times while eliminating positional drift, and Fang *et al.* [15] have developed a robust adaptive controller based on a reduced complexity electrochemical model. In both cases, these control systems have utilized noncontact laser displacement sensors as the displacement feedback mechanism, with dimensions much larger than the actuator being controlled. As the actuator approaches the microscale, the use of macroscale feedback sensors becomes less practical, particularly as the number of actuators and degrees of freedom increase. Sensing capacitance or thermal changes to a system can provide microscale displacement feedback [16], [17], but applying these techniques to trilayer conducting polymer actuators can prove difficult or impractical given the bending motion produced and potential working environments. Bending displacement sensors based on the trilayer actuator structure may be a potential solution [18], but require further development.

This paper presents the first application of an inversion-based feedforward control system to a conducting polymer actuator. This approach is taken because it can control tip position without the use of a feedback sensor, making it suitable for applications where displacement feedback is impractical. A model for actuator displacement was first identified and then inverted to calculate the feedforward input signal required to achieve a specified output displacement. This technique was able to improve the displacement performance of the conducting polymer actuator by 26 times, as measured against a feedforward-gain-controlled actuator, while maintaining acceptable positional accuracy. Dynamic performance has also been improved, with unity gain achieved and phase error reduced at low frequencies, as compared to the feedforward-gain control system. The ability of the control system to deal with changes in applied load, changes in geometry, and extended actuation has also been identified.

II. Experimental Setup

A. Trilayer Bender Actuator Structure

A laminated bending actuator, or trilayer, is the device used in this study, comprising a porous inactive substrate upon which

Manuscript received October 30, 2008; revised January 31, 2009. First published August 18, 2009; current version published November 18, 2009. Recommended by Technical Editor Z. Lin.

S. W. John is with the School of Mechanical, Materials and Mechatronic Engineering, University of Wollongong, Wollongong, N.S.W. 2522, Australia (e-mail: swj56@uow.edu.au).

G. Alici is with the School of Mechanical, Materials and Mechatronic Engineering and the ARC Center of Excellence on Electromaterials Science, University of Wollongong, Wollongong, N.S.W. 2522, Australia (e-mail: gursel@uow.edu.au).

C. D. Cook is with the Faculty of Engineering, University of Wollongong, Wollongong, N.S.W. 2522, Australia (e-mail: ccook@uow.edu.au).

Color versions of one or more of the figures in this paper are available online at http://ieeexplore.ieee.org.

Digital Object Identifier 10.1109/TMECH.2009.2020732

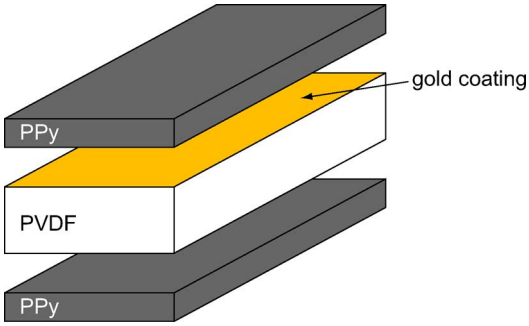

Fig. 1. Exploded structure of the trilayer bending actuator. The PVDF substrate is coated on both sides by a very thin gold coating, upon which the PPy is electrochemically deposited.

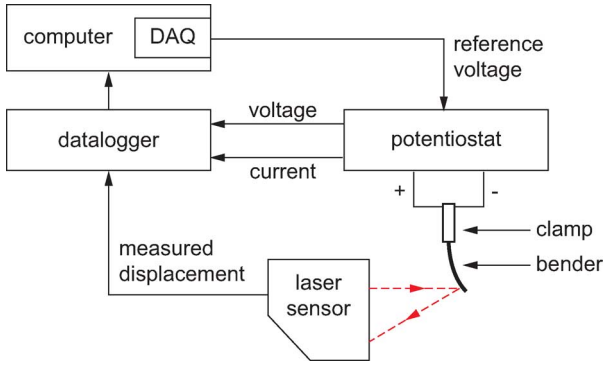

Fig. 2. Schematic of the experimental setup.

the conducting PPy is deposited (Fig. 1). The porous substrate used in this study is poly(vinylidene fluoride) (PVDF) that stores electrolyte and electrically separates the two PPy layers, which allows the actuator to operate in air.

Conducting polymer actuators have been described as electrochemomechanical devices, which convert electrical energy into mechanical work via the chemical domain. Applying a voltage across the device shifts the amount of charge in each conducting polymer layer, thus forcing mobile ionic species to move throughout the actuator structure to return the system to electroneutrality. The movement of ionic species [19] and the concomitant solvent movement [20] are linked to changes in the volume of the conducting polymer. If the two PPy layers have different levels of charge, they will also have differing volumes, thus causing the trilayer actuator structure to bend and generating mechanical work. A detailed review of the actuation processes of conducting polymers has been performed by Smela [2].

Input voltages are typically restricted below 2 V [21], but may be increased to a maximum of approximately 5 V. The application of constant voltages beyond 5 V can result in rapid deterioration of actuation performance [22], [23] due to overoxidation of the polypyrrole; however, very short high voltage pulses can be applied without significant damage [10].

B. Trilayer Bender Actuator Synthesis

The trilayer bending actuators were produced using a galvanostatic process, which has been reported previously [9], [24]. The substrate, PVDF (Immobilon-P, Millipore), had an initial thickness of 127 μm, and was sputter-coated with a thin layer of gold to make it electrically conductive. The gold-coated PVDF was cut to size and secured in a holding frame, then placed in the polymerization solution, comprising 0.1 M Pyrrole (Merck), 0.1 M lithium bis(triflouromethanesulfonyl)imide (Li^+TFSI^-, 3 M), and 1wt.% water in the solvent propylene carbonate (PC, Sigma–Aldrich). The gold-coated PVDF formed the working electrode in the cell, while a stainless steel mesh was used for the counter electrode. The cell was cooled to -35 °C and a constant current of 0.1 mA/cm^2 was applied for 12 h, thereby producing approximately 22 μm of PPy on each side. On completion of the polymerization, PPy-coated PVDF was removed from the frame, washed with acetone, and stored in the actuation solution of 0.1 M Li^+TFSI^- in PC. Benders were then cut from the bulk sheet, as required, using a sharp scalpel.

C. Displacement Measurement System

A custom-built experimental system was used to apply an arbitrary voltage input to trilayer bender actuator and to measure its response (Fig. 2). The actuator input voltage signal was first predetermined using the computer, then generated by a DAQ (NI6229) and amplified using a potentiostat (eDAQ, model EA161) operating in two-electrode mode. A noncontact laser displacement sensor (microepsilon, model NCDT-1700-10) was used to measure the displacement of the actuator and was focused at a constant position of 1.0 mm from the free end, unless otherwise noted. The resolution of the laser displacement sensor was 0.5 μm, but the measurement electronics introduces a 2-ms delay. A datalogger (eDAQ, model ED821) recorded the voltage signal applied to the trilayer actuator, the associated current drawn, and the displacement voltage signal from the laser displacement sensor at a sampling rate of 1 kHz.

III. Uncompensated Displacement

To identify the uncompensated displacement of a bender actuator, several step voltages were applied to a 10-mm-long, 2-mm-wide sample (Fig. 3). The displacement of the trilayer bender was found to be linear after 5 s of applied voltage (Fig. 4), and this relationship can be used to model the steady-state position; however, this proportional model provides no information about the dynamic displacement.

The relationship between the input voltage and steady-state displacement can be used as the basis of a feedforward-gain control system, as shown in Fig. 5, and described by (1), where $Y_d(s)$ is the desired displacement input, K is the gain, $G(s)$ is the actuator, and $Y(s)$ is the displacement output. The gain K is determined from the relationship between the steady-state displacement and input voltage, which is equivalent to the slope of the trendline shown in Fig. 4, and it is 0.11 V/mm here. Note that the gain K may change between actuator devices, due to variability between the samples. The control system determines the input voltage $U_c(s)$ required to achieve the desired steady-state displacement $Y_d(s)$, but as no dynamic compensation is

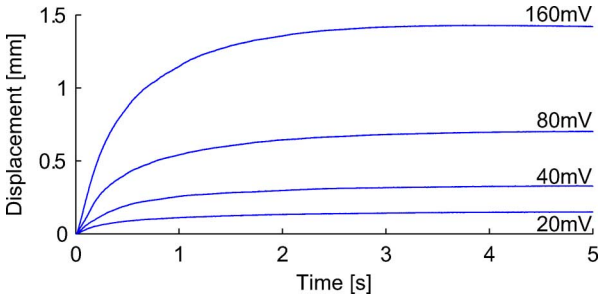

Fig. 3. Displacement of a 10-mm-long, 2-mm-wide bender in response to multiple input step voltage amplitudes.

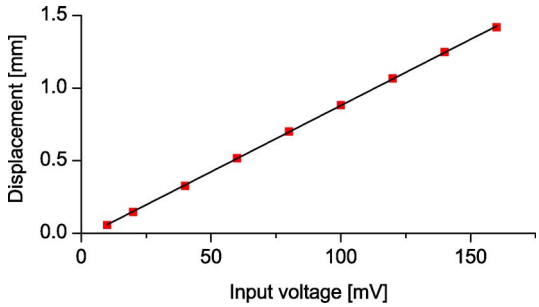

Fig. 4. Displacement of a trilayer bender after 5 s as a function of input voltage. A linear trendline has been fitted, $y = 0.0091x + 0.032$.

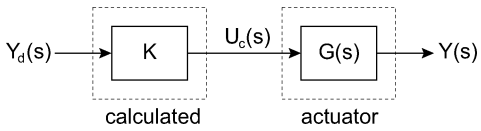

Fig. 5. Schematic of the feedforward-gain control system.

performed, there is no improvement in its performance

$$Y(s) = \underbrace{Y_d(s)K}_{U_c(s)} G(s) \tag{1}$$

$$\hat{G}(s) = \frac{Y(s)}{U(s)} = k\frac{\prod_{m=1}^{5}(s - z_m)}{\prod_{n=1}^{6}(s - p_n)}. \tag{2}$$

IV. Frequency-Response Model

The relation between the input voltage u and the output displacement y of the trilayer bender has been experimentally measured as a function of frequency (Fig. 6).

Considering the relationship between the input and output to be a "black box," an empirical sixth-order transfer function of the form (2) was fitted to the experimentally identified frequency response using an iterative search algorithm (solid line in Fig. 6), with $k = 0.29$ and the fitted poles and zeros, as presented in Table I. The accuracy of the fit is high, such that the model can be used to simulate bender displacement in response to step voltage inputs (Fig. 7) and dynamic inputs [24]. Given the accuracy of the model in simulating the displacement behavior of the actuator and it is minimum phase, the model is suitable for use in an inversion-based feedforward control system.

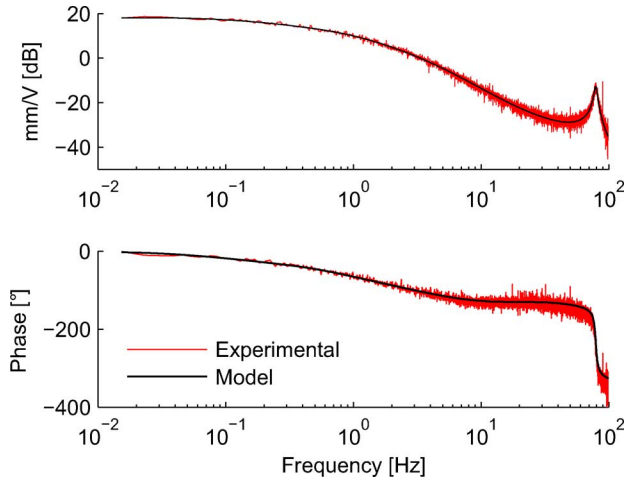

Fig. 6. Frequency response of a trilayer bender. A transfer function model has also been fitted to the response (solid line).

TABLE I
Fitted Model Parameters

m, n	z_m	p_n
1	-1.33	-0.88
2	-125.7	-4.58
3	-1619	-34.0
4	-1282+1229i	-898
5	-1282-1229i	-13.6+498.4i
6		-13.6-498.4i

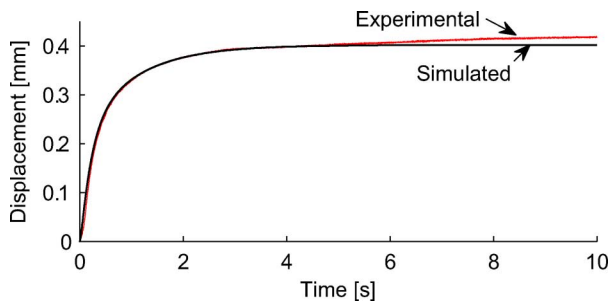

Fig. 7. Experimentally identified and model-simulated displacement in response to a 50-mV step input.

V. Inversion-Based Feedforward Control

A. Principle of Operation

For a given system $Y(s) = U(s)G(s)$, where $U(s)$ is the input and $Y(s)$ is the output, it follows that the ideal input signal to achieve a desired output signal is $U_c(s) = Y_d(s)\hat{G}^{-1}(s)$, as the inverse plant model $\hat{G}^{-1}(s)$ will compensate for the plant dynamics (3). The displacement model (2) obtained in Section IV will be used to develop the inversion-based feedforward control system.

B. Development of the Controller

The transfer function obtained for a 10-mm-long, 2-mm-wide trilayer has been inverted by swapping the poles and zeros, and taking the reciprocal of the gain, with the theoretical frequency response presented in Fig. 8. The exact inverted transfer function

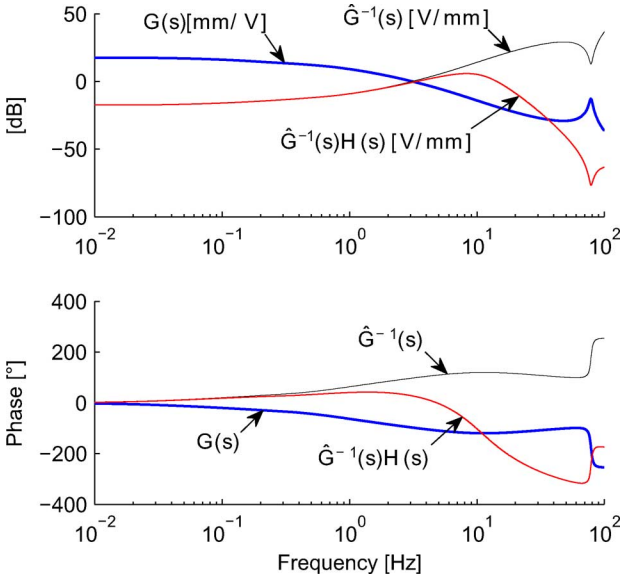

Fig. 8. Frequency response of the example system $G(s)$, the inverted system with $[\hat{G}^{-1}(s)H(s)]$, and without $[\hat{G}^{-1}(s)]$ filtering applied. The gain of $G(s)$ has units of millimeters per volt, while both inverted systems have units of volts per millimeter.

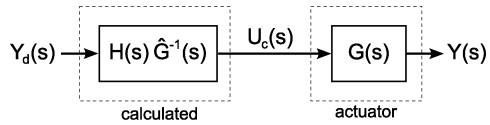

Fig. 9. Schematic diagram of the practical inversion-based feedforward control system.

$\hat{G}^{-1}(s)$ can be obtained by direct inversion, as all poles and zeros are on the left-hand side of the s-plane, but the result is unrealizable as it has a greater number of zeros than poles ($m > n$), generating an infinite gain at high frequencies. As such, it cannot be used in practical systems.

To use the inverted transfer function in a practical control system, low-pass filtering $[H(s)]$ has been applied to limit the gain at high frequencies and make the system realizable, as shown in the filtered frequency response $[\hat{G}^{-1}(s)H(s)$ in Fig. 8] and schematically in Fig. 9. The characteristics of the low-pass filter will influence the behavior of the system (4), as an increase in high-frequency filtering results in the reduced compensation of high-frequency dynamics, while also reducing the magnitude of the input signal.

For the purposes of this study, a Bessel filter has been utilized for $H(s)$, as it is causal with a controllable order and cutoff frequency. The filter parameters used for all tests in this paper have been of fifth order, with a 10 Hz cutoff frequency, as this sufficiently limits the high-frequency gain and the magnitude of the feedforward input signal, without excessively changing the dynamics of the inverted model.

C. Step Response

The input voltage calculated by the inversion-based feedforward control system, drawn current, and resulting displacement

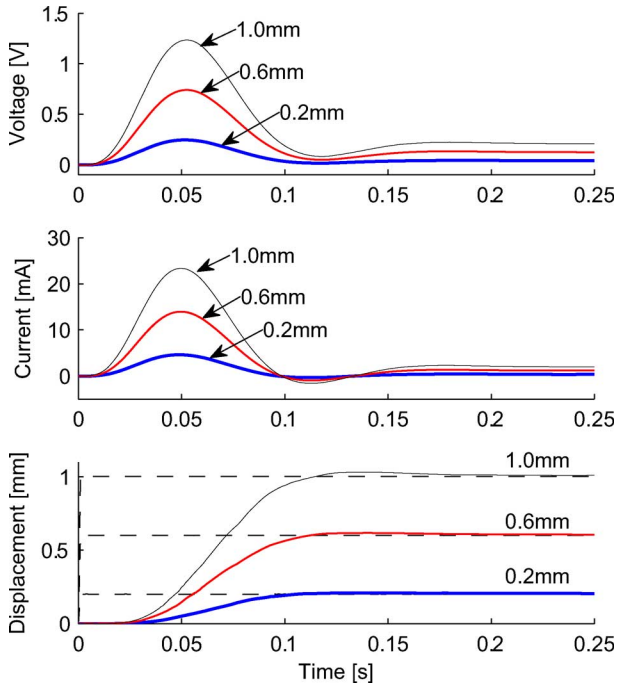

Fig. 10. Voltage, current, and displacement for a 10-mm long, 2-mm-wide trilayer actuator under inversion-based feedforward control. The input displacement to the control system is also shown (dotted line in bottom panel).

TABLE II
INVERSION-BASED FEEDFORWARD-CONTROLLED STEP DISPLACEMENT PERFORMANCE

Input displacement [mm]	Peak voltage [V]	Peak current [mA]	Rise time [ms]	Steady state error [%]	Delay [ms]
0.2	0.24	4.6	55	1.9	65
0.4	0.49	9.3	56	1.0	64
0.6	0.74	14.0	59	1.4	65
0.8	0.99	18.7	60	2.6	66
1.0	1.23	23.3	60	2.3	65

of a 10-mm-long, 2-mm-wide trilayer bender is presented in Fig. 10 for three different step input amplitudes. As summarized in Table II, the displacement output, peak input voltage, and peak current also remained linear with desired displacement, while the rise time and delay are similar for all tests.

The uncompensated step responses have been experimentally identified for the same 10-mm-long, 2-mm-wide trilayer bender, and are presented with the inversion-based controlled step responses in Fig. 11, with displacement characteristics presented in Table III. The average rise time under inversion-based feedforward control was 58 ms, which represents an improvement of 26 times over the uncompensated system; this could be further improved by optimizing the Bessel filter parameters or calculation of the optimal inverse. The delay is also improved by an average of 3.9 times over the uncompensated system. The peak voltage and current were increased under inversion-based feedforward control compared to the uncompensated system; however, the highest peak voltage applied to the actuator by the control system was 1.23 V, which remains within the safe

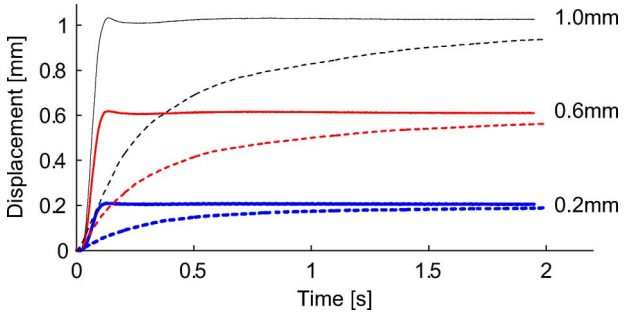

Fig. 11. Comparison of the first 2 s of feedforward-gain-controlled (dotted) and feedforward-inversion-based controlled (solid) step responses for inputs of 0.2, 0.6, and 1.0 mm.

TABLE III
FEEDFORWARD-GAIN-CONTROLLED STEP DISPLACEMENT PERFORMANCE

Input displacement [mm]	Peak voltage [V]	Peak current [mA]	Rise time [ms]	Steady state error [%]	Delay [ms]
0.2	0.03	0.8	1445	1.7	242
0.4	0.06	1.5	1590	-0.2	243
0.6	0.10	2.3	1429	-0.1	256
0.8	0.13	3.1	1542	-0.3	257
1.0	0.16	3.8	1582	1.2	262

operating range

$$Y(s) = \underbrace{Y_d(s)\hat{G}^{-1}(s)}_{U_c(s)} G(s) \tag{3}$$

$$Y(s) = \underbrace{Y_d(s)H(s)\hat{G}^{-1}(s)}_{U_c(s)} G(s) = Y_d(s)H(s). \tag{4}$$

D. Dynamic Response

The dynamic displacement response of an inversion-based controlled 10-mm-long, 2-mm-wide trilayer bender was measured in response to two mixed sinusoidal signals—sine A ($y_d = 0.5\sin(0.2\pi t) + 0.02\sin(2\pi t)$ Fig. 12) and sine B ($y_d = 0.5\sin(2\pi t) + 0.02\sin(20\pi t)$, Fig. 13). The gain and phase shift of the component frequencies were extracted from the displacement output under inversion-based control and are shown in Table IV. The output of the system is also compared to the simulated actuator response under the feedforward-gain control system.

The output displacement of the inversion-based controlled system was found to be within 5% of unity gain for the input frequencies of 0.1 and 1 Hz, indicating that the low-pass filter did not affect the output at these frequencies. The attenuation of the displacement at 10 Hz is attributable to the low-pass filter, as it is equal to the theoretical attenuation of the low-pass Bessel filter at that frequency. The phase shift is also shown to improve over the uncompensated system at all frequencies tested.

E. Loading Effect

To simulate the effect of loading on the trilayer bender, the step displacement response of a 10-mm-long, 2-mm-wide trilayer bender was identified as the tip load applied to the actuator was increased (Fig. 14) to a maximum of 22.3 mg. The mass of the trilayer bender is approximately 5.2 mg.

The application of mass, up to 4.3 times that of the actuator, caused a reduction in the rise time of the step response, and variation in the steady-state error. The overshoot can also

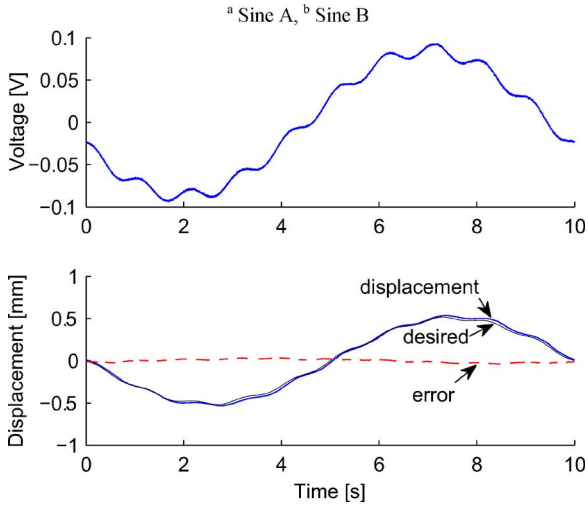

Fig. 12. Dynamic displacement response of a 10-mm-long, 2-mm-wide trilayer bender under feedforward inversion-based control in response to an input of $y_d = 0.5\sin(0.2\pi t) + 0.02\sin(2\pi t)$.

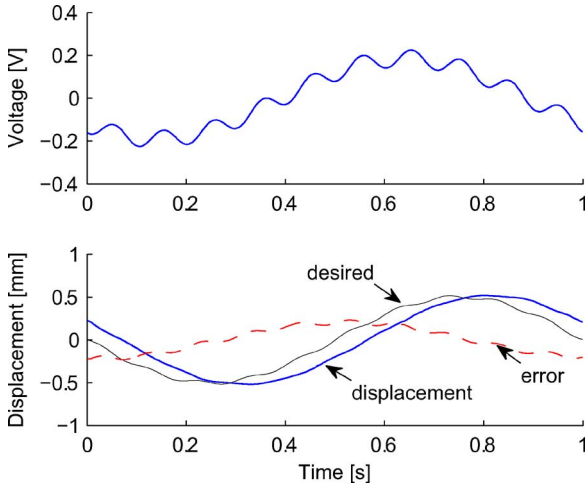

Fig. 13. Dynamic displacement response of a 10-mm-long, 2-mm-wide trilayer bender under feedforward inversion-based control in response to an input of $y_d = 0.5\sin(2\pi t) + 0.02\sin(20\pi t)$.

TABLE IV
DYNAMIC RESPONSE OF FEEDFORWARD-CONTROLLED ACTUATOR

Input Frequency [Hz]	Inversion-based controller		Feedforward gain controller	
	Gain [mm/mm]	Phase shift [°]	Gain [mm/mm]	Phase shift [°]
0.1[a]	1.04	-2.3	0.85	-20.7
1.0[a]	1.00	-23.9	0.39	-62.4
1.0[b]	1.03	-25.0	0.39	-62.4
10[b]	0.35	-55.6	0.03	-120.1

[a]Sine A; [b]sine B.

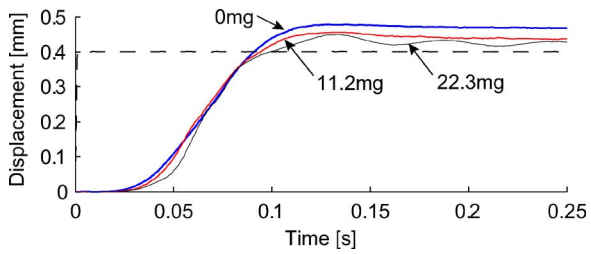

Fig. 14. Comparative displacements of 10-mm-long, 2-mm-wide trilayer bender in response to a 0.4 mm step input and three different tip loadings.

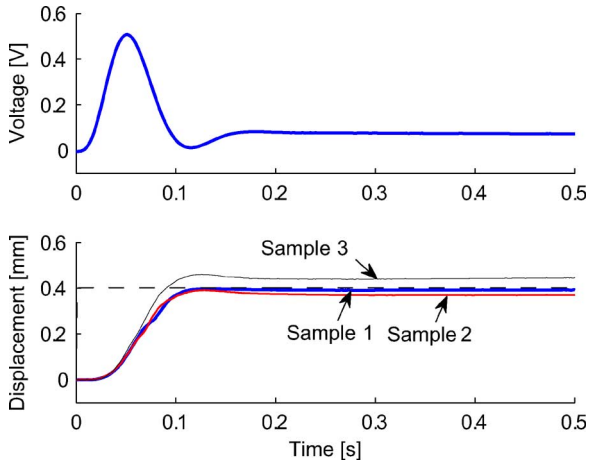

Fig. 15. Response of three trilayer bender actuators to a 0.4-mm step displacement, obtained using the same transfer function model.

be seen to increase, and oscillation is visible in the 22.3 mg step response (Fig. 14), due to the resonant frequency diverging from the model when loaded [25]. The control system is shown to handle changes in load, as the performance remains within acceptable ranges.

F. Repeatability

To identify the performance of the inversion-based control system across multiple actuators of similar dimension, the model for a 10-mm-long, 2-mm-wide trilayer bender (sample 1) was developed and applied to three actuators cut to the same length and width (samples 1–3 in Fig. 15). The laser was focused at a constant 9.0 mm from the base of the clamp for all three samples tested to minimize the effect of any variation in actuator length on the measured displacement. The frequency response of the trilayer displacement was identified for all three actuators, and is shown in Fig. 16, with the resonant frequency and step-response characteristics summarized in Tables V and VI.

The same model used to calculate the feedforward control signal could not be effectively applied in practice to three different actuator samples of similar dimensions, with variable steady-state displacements produced. While care was taken to try and obtain identical dimensions when cutting the actuators, the resonant frequencies of the three actuators were found to differ, indicating they were not sufficiently close to the same length or mass [25]. Unless the geometric control of the trilayer benders can be improved, a model will have to be tailored for each individual actuator.

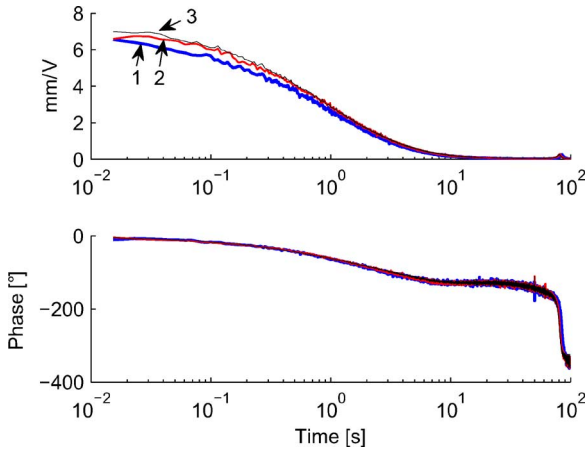

Fig. 16. Comparison of experimentally identified frequency responses for three 10-mm-long, 2-mm-wide trilayer bender samples.

TABLE V
PERFORMANCE OF ACTUATOR 0.4-mm STEP DISPLACEMENT UNDER LOAD

Applied load [mg]	Peak voltage [V]	Rise time [ms]	Overshoot [%]	Steady state error [%]
0	0.47	57	2.4	14.3
5.6	0.47	53	2.2	4.7
11.2	0.47	50	5.8	6.9
22.3	0.47	45	5.9	5.2

TABLE VI
RESPONSE OF THREE ACTUATOR SAMPLES TO IDENTICAL 0.4-mm STEP INPUT

Sample number	Peak voltage [V]	Peak current [mA]	Rise time [ms]	Steady state error [%]	Resonant frequency [Hz]
1	0.51	10.7	56	-2.9	84.4
2	0.51	10.1	52	-8.7	81.3
3	0.51	9.9	52	9.7	80.5

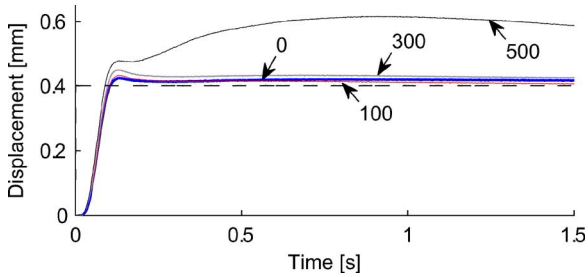

Fig. 17. Displacement response of the 1st, 100th, 300th, and 500th cycle of a 10-mm-long, 2-mm-wide trilayer bender to a repeated 0.4 mm step input.

G. Multiple Actuation Cycles

A step-response signal was applied to the trilayer bender for 500 cycles to identify the change in the response with time, as shown in Fig. 17. Each cycle lasted 10 s, consisting of a forward displacement signal of +0.4 mm, 2 s of 0 mm, 2 s of −0.4 mm, and 4 s of 0 mm.

The change in response of a trilayer bender actuator to repeated short-term step displacements was found to be minimal over the first 300 cycles (Fig. 17), increasing to over 55% (or 0.22 mm) by the 500th cycle. By the 500th cycle, the PVDF had

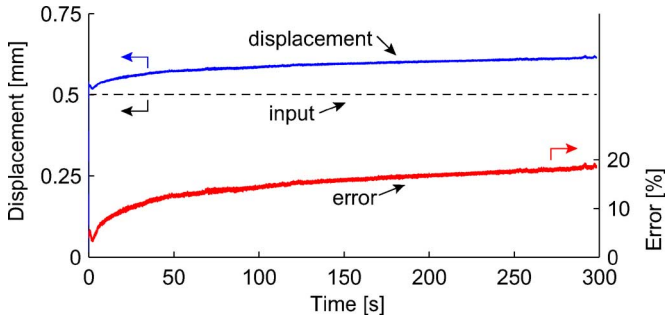

Fig. 18. Step displacement of a 10-mm-long, 2-mm-wide trilayer bender in response to a 0.5 mm step displacement input, as measured over 300 s. The error between the specified and actual tip displacement is also shown.

become visible as a white band down the center of the actuator, indicating that drying had occurred. Evaporation of solvent from the electrolyte has been previously reported for trilayer actuators [15], [26], shifting the electrochemical behavior away from the initially modeled state.

H. Extended Step Response

The step displacement response of a trilayer bender was measured for a 10-mm-long, 2-mm-wide trilayer actuator over 300 s (Fig. 18). The displacement error is approximately 4% immediately after steady state is reached, which increases with time to 18.5% at 300 s. The control voltage calculated by the feedforward control system did not return to zero after the initial pulse, remaining at 78 mV for the duration of the step.

The positional error of an extended step input (Fig. 18) was found to increase steadily with time, which may be linked to inaccuracies in the dc gain of the model over longer time periods. The change in electrochemical state of polymer is also known to progress through the film with time [27], [28], and the continued dc voltage may further contribute to longer term displacement.

VI. Discussion and Conclusion

This paper has presented the successful implementation of an inversion-based feedforward control system, applied to a bending trilayer actuator for the first time. This technique was capable of improving the step and dynamic performance of a trilayer actuator without the use of feedback.

An empirical transfer function model structure was identified and fitted to the experimentally obtained trilayer actuator frequency response. This model was able to accurately represent the actuator displacement up to the resonant frequency and could be used to simulate the displacement of the actuator in response to arbitrary inputs.

The inversion-based feedforward control system, based on the transfer function displacement model, was shown to improve the response time of the trilayer bender actuator without the use of a feedback sensor, decreasing the rise time by an average of 26 times over the feedforward-gain control system. Typical rise times measured throughout this paper were below 60 ms, where the fifth-order low-pass Bessel filters were used. In comparison, a tuned PID control system applied to the same type of trilayer bender actuator was able to achieve a 0%–100% rise time of 132 ms [14]. The response to sinusoidal displacements was also improved under inversion-based control, with phase shift reduced in all cases, as compared to the feedforward-gain control system. This indicates that the inversion-based feedforward control system is capable of overcoming the slow response traditionally associated with conducting polymer bending actuators [7] without chemical modification.

The inversion-based feedforward control system was found to remain stable when applied mass was increased, with step-response performance maintained as the load on the actuator was raised well beyond its own mass. The control system was not consistent when applied to a different actuator, as slight variations in the mass and geometry were sufficient to vary the output. This indicates that the inverted model must be tailored to each individual actuator, until more repeatable manufacturing techniques are developed.

The steady-state displacement error changed throughout the paper, indicating some inaccuracy in the low frequency and dc gain of the fitted models. This was evident across all short-term and the long-term displacement tests. A constant gain could be incorporated into the inversion-based feedforward controller and tuned to minimize the steady-state error at short time periods; however, this may not be sufficient to reduce the error over longer term periods. The use of a feedforward control system is less complex to implement than a feedback control system, but it cannot identify or compensate for steady-state error, external disturbances, or unmodeled system changes that occur to the actuator. The decision to implement a feedforward control system will require consideration of these issues, and it is likely to be best suited to applications where feedback is difficult or impractical, such as a multiple degree of freedom microscale robotic device.

The displacement performance in response to short actuation cycles was seen to be constant over the first 300 cycles, but diverged up to the 500th cycle, most likely due to the evaporation of solvent from the actuator structure. Reducing the solvent evaporation, through the use of encapsulation [29] or less volatile ion sources, such as ionic liquids [30], may stabilize the system and improve the long-term response of the controlled actuator, but these currently come at the cost of reduced displacement performance.

The inversion-based control technique applied in this paper has been applied to a conducting polymer actuator for the first time, and has been demonstrated to improve the step and dynamic displacement of a conducting polymer trilayer bender over a feedforward-gain-controlled actuator. The inversion-based controller has been shown to be able to deal with changes in load, and performance was consistent over the first 100 cycles. As this performance increase has been achieved without the use of feedback, the inversion-based approach shows potential for applications where implementing feedback is impractical, such as conducting polymer-based micro- and nanoscale manipulation systems. Future work will consider the use of physics-based models, such as [31], for the inversion-based feedforward control system, as this has a number of potential advantages over the empirical model, including geometric scaling. However, before existing physics-based models can be incorporated into a feedforward control system, their accuracy must first be

improved. Novel feedback sensors and strategies appropriate for microscale bending conducting polymer actuators will also be investigated.

ACKNOWLEDGMENT

The authors would like to thank the members of the Intelligent Polymer Research Institute at the University of Wollongong for the kind assistance in the preparation of trilayer actuators.

REFERENCES

[1] R. H. Baughman, "Conducting polymer artificial muscles," *Synth. Metals*, vol. 78, pp. 339–353, 1996.
[2] E. Smela, "Conjugated polymer actuators for biomedical applications," *Adv. Mater.*, vol. 15, pp. 481–494, 2003.
[3] E. Smela, "Microfabrication of PPy microactuators and other conjugated polymer devices," *J. Micromech. Microeng.*, vol. 9, pp. 1–18, 1999.
[4] G. Alici and N. N. Huynh, "Performance quantification of conducting polymer actuators for real applications: A microgripping system," *IEEE/ASME Trans. Mechatronics*, vol. 12, no. 1, pp. 73–84, Feb. 2007.
[5] E. H. Jager, O. Inganas, and I. Lundstrom, "Microrobots for micrometer-size objects in aqueous media: Potential tools for single-cell manipulation," *Science*, vol. 288, pp. 2335–2338, 2000.
[6] G. Alici, V. Devaud, P. Renaud, and G. Spinks, "Conducting polymer microactuators operating in air," *J. Micromech. Microeng.*, vol. 19, pp. 025017-1–025017-9, 2009.
[7] G. Alici and N. N. Huynh, "Predicting force output of trilayer polymer actuators," *Sens. Actuators A*, vol. 132, pp. 616–625, 2006.
[8] E. Smela, M. Kallenbach, and J. Holdenried, "Electrochemically driven polypyrrole bilayers for moving and positioning bulk micromachined silicon plates," *J. Microelectromech. Syst.*, vol. 8, pp. 373–383, 1999.
[9] Y. Wu, G. Alici, G. M. Spinks, and G. G. Wallace, "Fast trilayer polypyrrole bending actuators for high speed applications," *Synth. Metals*, vol. 156, pp. 1017–1022, 2006.
[10] J. D. Madden, R. A. Cush, T. S. Kanigan, and I. W. Hunter, "Fast contracting polypyrrole actuators," *Synth. Metals*, vol. 113, pp. 185–192, 2000.
[11] S. Hara, T. Zama, W. Takashima, and K. Kaneto, "TFSI-doped polypyrrole actuator with 26% strain," *J. Mater. Chem.*, vol. 14, pp. 1516–1517, 2004.
[12] S. Hara, T. Zama, W. Takashima, and K. Kaneto, "Free-standing gel-like polypyrrole actuators doped with bis(perfluoroalkylsulfonyl)imide exhibiting extremely large strain," *Smart Mater. Struct.*, vol. 14, pp. 1501–1510, 2005.
[13] T. Zama, S. Hara, W. Takashima, and K. Kaneto, "Comparison of conducting polymer actuators based on polypyrrole doped with BF4−, PF6−, CF3SO3− and ClO4−," *Bull. Chem. Soc. Jpn.*, vol. 78, pp. 506–511, 2005.
[14] Q. Yao, G. Alici, and G. M. Spinks, "Feedback control of tri-layer polymer actuators to improve their positioning ability and speed of response," *Sens. Actuators A*, vol. 144, pp. 176–184, 2008.
[15] Y. Fang, X. Tan, and G. Alici, "Robust adaptive control of conjugated polymer actuators," *IEEE Trans. Control Syst. Technol.*, vol. 16, no. 4, pp. 600–612, Jul. 2008.
[16] D. J. Bell, T. J. Lu, N. A. Fleck, and S. M. Spearing, "MEMS actuators and sensors: Observations on their performance and selection for purpose," *J. Micromech. Microeng.*, vol. 15, pp. S153–S164, 2005.
[17] S. Devasia, E. Eleftheriou, and S. O. R. Moheimani, "A survey of control issues in nanopositioning," *IEEE Trans. Control Syst. Technol.*, vol. 15, no. 5, pp. 802–823, Sep. 2007.
[18] G. Alici, G. Spinks, J. D. W. Madden, Y. Wu, and G. G. Wallace, "Response characterisation of electroactive polymers as mechanical sensors," *IEEE/ASME Trans. Mechatronics*, vol. 13, no. 2, pp. 187–196, Apr. 2008.
[19] M. R. Ghandi, P. Murray, G. M. Spinks, and G. G. Wallace, "Mechanism of electromechanical actuation in polypyrrole," *Synth. Metals*, vol. 73, pp. 247–256, 1995.
[20] L. Bay, T. Jacobsen, and S. Skaarup, "Mechanism of actuation in conducting polymers: Osmotic expansion," *J. Phys. Chem. B*, vol. 105, pp. 8492–8497, 2001.
[21] J. D. W. Madden, B. Schmid, M. Hechinger, S. R. Lafontaine, P. G. A. Madden, F. S. Hover, R. Kimball, and I. W. Hunter, "Application of polypyrrole actuators: Feasibility of variable camber foils," *IEEE J. Ocean. Eng.*, vol. 29, no. 3, pp. 738–749, Jul. 2004.
[22] G. M. Spinks, L. Lu, G. G. Wallace, and D. Zhou, "Strain response from polypyrrole actuators under load," *Adv. Funct. Mater.*, vol. 12, pp. 437–440, 2002.
[23] G. M. Spinks, B. Xi, D. Zhou, V.-T. Truong, and G. G. Wallace, "Enhanced control and stability of polypyrrole electromechanical actuators," *Synth. Metals*, vol. 140, pp. 273–280, 2004.
[24] S. John, G. Alici, and C. Cook, "Frequency response of polypyrrole trilayer actuator displacement," in *Proc. Electroactive Polym. Actuators Devices (EAPAD) 2008*, San Diego, CA, pp. 69271T-1–69271T-8.
[25] S. John, G. Alici, and C. Cook, "Validation of a resonant frequency model for polypyrrole trilayer actuators," *IEEE/ASME Trans. Mechatronics*, vol. 13, no. 4, pp. 401–409, Aug. 2008.
[26] M. K. Andrews, M. L. Jansen, G. M. Spinks, D. Zhou, and G. G. Wallace, "An integrated electrochemical sensor-actuator system," *Sens. Actuators A, Phys.*, vol. 114, pp. 65–72, 2004.
[27] Y. Tezuka, S. Ohyma, T. Ishii, and K. Aoki, "Observation of propagation speed of conductive front in electrochemical doping process of polypyrrole films," *Bull. Chem. Soc. Jpn.*, vol. 64, pp. 2045–2051, 1991.
[28] X. Wang, B. Shapiro, and E. Smela, "Visualizing ion currents in conjugated polymers," *Adv. Mater.*, vol. 16, pp. 1605–1609, 2004.
[29] J. D. Madden, R. A. Cush, T. S. Kanigan, C. J. Brenan, and I. W. Hunter, "Encapsulated polypyrrole actuators," *Synth. Metals*, vol. 105, pp. 61–64, 1999.
[30] W. Lu, A. G. Fadeev, B. Qi, E. Smela, B. R. Mattes, J. Ding, G. M. Spinks, J. Mazurkiewicz, D. Zhou, G. G. Wallace, D. R. MacFarlane, S. A. Forsyth, and M. Forsyth, "Use of ionic liquids for pi-conjugated polymer electrochemical devices," *Science*, vol. 297, pp. 983–987, 2002.
[31] Y. Fang, X. Tan, Y. Shen, N. Xi, and G. Alici, "A scalable model for trilayer conjugated polymer actuators and its experimental validation," *Mater. Sci. Eng. C*, vol. 28, pp. 421–428, 2008.

Stephen W. John received the B.E. (with first-class honors) and Ph.D. degrees in mechatronics engineering from the University of Wollongong, Wollongong, Australia, in 2004 and 2009, respectively.

He was engaged in the field of the dynamic behavior of conducting polymer trilayer actuators. He is currently with the School of Mechanical, Materials and Mechatronic Engineering, University of Wollongong.

Gursel Alici received the Ph.D. degree in robotics from the Department of Engineering Science, Oxford University, Oxford, U.K., in 1993.

He is currently an Associate Professor of mechatronic engineering at the University of Wollongong, Wollongong, Australia. His current research interests include intelligent mechatronic systems involving mechanisms/serial/parallel robot manipulators, micro-/nanorobotic manipulation systems, and modeling, analysis, characterization, control, and micro-/nanofabrication of conducting polymer actuators and sensors for robotic and bio-inspired applications.

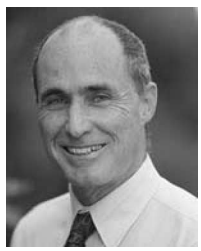

Christopher D. Cook received the B.Sc. and B.E. degrees from The University of Adelaide, Adelaide, Australia, in 1971 and 1972, respectively, and the Ph.D. degree in the modeling and control of electrical machines from The University of New South Wales, Kensington, Australia, in 1976.

He was with GEC Marconi Avionics, Rochester, U.K., where he was engaged in the design of computers for various aerospace applications. After three years, he returned to Australia to work for GEC as the Technical Manager of the Automation and Control Division in the area of industrial automation. In 1983, he joined the University of Wollongong, Wollongong, Australia, where he became a Professor of electrical engineering in 1989, was appointed as the Dean of Engineering in 2002, and is engaged in industrial automation and power engineering.